



**HAL**  
open science

# Dynamic strain ageing and the mechanical response of alloys

L. Kubin, Y. Estrin

► **To cite this version:**

L. Kubin, Y. Estrin. Dynamic strain ageing and the mechanical response of alloys. Journal de Physique III, 1991, 1 (6), pp.929-943. 10.1051/jp3:1991166 . jpa-00248641

**HAL Id: jpa-00248641**

**<https://hal.science/jpa-00248641>**

Submitted on 4 Feb 2008

**HAL** is a multi-disciplinary open access archive for the deposit and dissemination of scientific research documents, whether they are published or not. The documents may come from teaching and research institutions in France or abroad, or from public or private research centers.

L'archive ouverte pluridisciplinaire **HAL**, est destinée au dépôt et à la diffusion de documents scientifiques de niveau recherche, publiés ou non, émanant des établissements d'enseignement et de recherche français ou étrangers, des laboratoires publics ou privés.

Classification

*Physics Abstracts*

81.40L — 62.20F — 03.40K

## Dynamic strain ageing and the mechanical response of alloys

L. P. Kubin <sup>(1)</sup> and Y. Estrin <sup>(2)</sup>

<sup>(1)</sup> CNRS-ONERA (OM), 29 Av. de la Div. Leclerc, BP 72, 92322 Châtillon Cedex, France

<sup>(2)</sup> T.U. Hamburg-Harburg, Eissendorfer Str. 42, 2100 Hamburg 90, F.R.G.

*(Received 17 March 1990, accepted 4 September 1990)*

**Résumé.** — Les mécanismes de vieillissement statique et dynamique qui sont caractéristiques des alliages dilués aux températures intermédiaires sont rappelés. L'accent est mis sur la réduction de ductilité qui résulte de la réduction de la sensibilité à la vitesse provoquée par le vieillissement dynamique. L'influence de la déformation et de la vitesse de déformation sur le vieillissement statique et dynamique ainsi que sur l'effet Portevin-Le Châtelier sont discutées et illustrées par des exemples portant sur divers alliages, en particulier les alliages avancés à base d'aluminium.

**Abstract.** — The mechanisms of static and dynamic strain ageing which occur in dilute alloys at moderate temperatures are briefly surveyed. Emphasis is put on the reduction of ductility which follows from the reduction in strain rate sensitivity caused by dynamic strain ageing. Strain and strain rate effects associated with static and dynamic strain ageing and with the Portevin-Le Châtelier effect are discussed with reference to a variety of alloys, in particular to advanced aluminium based alloys.

### 1. Introduction.

Dynamic strain ageing (DSA), static strain ageing (SSA) and the Portevin-Le Châtelier (PLC) effect are related phenomena which occur in dilute alloys at medium temperatures. Their detrimental effect on the mechanical performance of materials has been noticed already long ago. The underlying physical mechanisms have been the object of many academic studies and of some long-standing controversies. In the last decade the degree of understanding of discontinuous plastic flow (the PLC effect) has significantly advanced through a better modelling of the causes and consequences of the instability mechanisms. In parallel, the mechanisms of static and dynamic strain ageing have been reexamined and earlier interpretations have been revised. The elaboration of new classes of metallic alloys which also happen to exhibit these phenomena has caused a revival of interest to them, but the strong influence that solute species may have on the mechanical response is still largely underestimated or even ignored. This is particularly the case with DSA effects which do not manifest themselves as serrations on the stress strain curves, so that they can easily remain unnoticed.

This brief survey focusses on the following points. DSA, whose microstructural aspects are recalled in section 2, is a quite general phenomenon. Its occurrence is associated with a few

characteristic features, whatever the alloy considered, in particular with a significant reduction in the strain rate sensitivity (SRS). In section 3 the relation between the SRS and the ductility is examined through several practical examples. The strain dependence of DSA and SSA is considered in section 4, together with the critical strains for the PLC effect. Section 5 deals with strain rate effects, and an excursion is made into a related domain *viz.* that of stick-slip and solid friction in composite materials. In what follows we will not refer extensively to the bulk of existing literature, most of the examples illustrating recent results obtained on advanced materials, particularly aluminium based alloys. More detail can be found in two recent articles which review experimental and theoretical aspects, recent advancements and questions still under investigation [1, 2].

## 2. Basic mechanisms.

At temperatures of the order of  $0.3 T_m$  ( $T_m$ : melting temperature), solute atoms are able to diffuse over short distances and to pin mobile dislocations. A kind of resonance phenomenon occurs when the mobility of the solute species is of the same order as the dislocation velocity. In the early models, dislocations were assumed to move in a viscous manner. This led to a numerical inconsistency, i.e., a too low value of solute diffusivity in particular in substitutional alloys. To resolve this inconsistency, Cottrell [3] proposed that the diffusivity of substitutional solutes is enhanced by vacancies created during plastic flow in excess of thermal equilibrium. Classically, this vacancy concentration is assumed to increase monotonically with strain:  $c_v \approx 10^{-4} \varepsilon$  [4]. More generally, some power of strain is often assumed.

In more recent elaborations, starting with the work of McCormick [5] and van den Beukel [6], dislocations were assumed to move in a jerky manner. Thermally activated jumps through forest obstacles alternate in time with free-flight motion between two such obstacles. In this view, DSA occurs during a waiting time, i.e., while the dislocations are temporarily arrested by other (« forest ») dislocations piercing through their slip plane. According to some authors, including van den Beukel [6], the « vacancy hypothesis » is still needed to account for the properties of substitutional alloys, while for some others [7, 8] a transfer of solute atoms to the pinning points can occur by pipe diffusion along forest dislocations. Arguments have been presented in favour of one or the other of these two hypotheses [9] but no crucial proof has been delivered as yet. We return to this question in section 4.

According to Orowan's law, the applied strain rate can be written in the form :

$$\dot{\varepsilon} = \rho_m b (\lambda / t_w) = \Omega / t_w, \quad (1)$$

where  $\rho_m$  is the density of mobile dislocations,  $b$  is the magnitude of their Burgers vector,  $\lambda$  is the mean distance between forest obstacles, related to the density  $\rho_f$  of forest dislocations *via*  $\lambda = \rho_f^{-1/2}$  and  $t_w$  is the waiting time associated with the thermally activated cutting through forest obstacles. The quantity  $\Omega = b \rho_m \rho_f^{-1/2}$  is the elementary strain increment obtained when all the mobile dislocations simultaneously undergo a successful activation event. Assuming for the moment that  $\Omega$  is a constant, the waiting time is inversely proportional to the strain rate. Figure 1 shows a simple diagrammatic explanation of dynamic strain ageing effects (after Kocks [10]). The glide resistance is drawn as a function of the waiting time or of the applied strain rate and it is made up of two contributions. One (activation) accounts for the normal activation of flow processes and it decreases with increasing waiting time or decreasing strain rate. The second one (ageing) describes the diffusion of solute atoms towards the arrested dislocations and the resulting hardening which is usually taken to be a function of  $c$  and  $D t_w$ , where  $c$  is the volume concentration of solute atoms and  $D$  their diffusion coefficient. Given the temperature and the concentration, ageing effects increase with increasing waiting times and saturate to some maximum value (cf. Fig. 14, below).

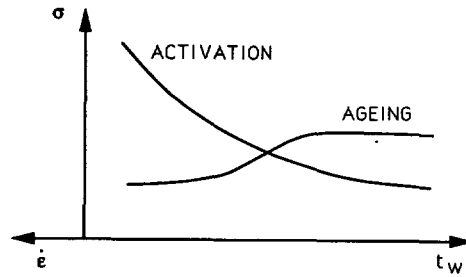


Fig. 1. — Decomposition of the glide resistance  $\sigma$  into two components, activation and aging, which have opposite dependences on strain rate,  $\dot{\epsilon}$ , or waiting time  $t_w$ .

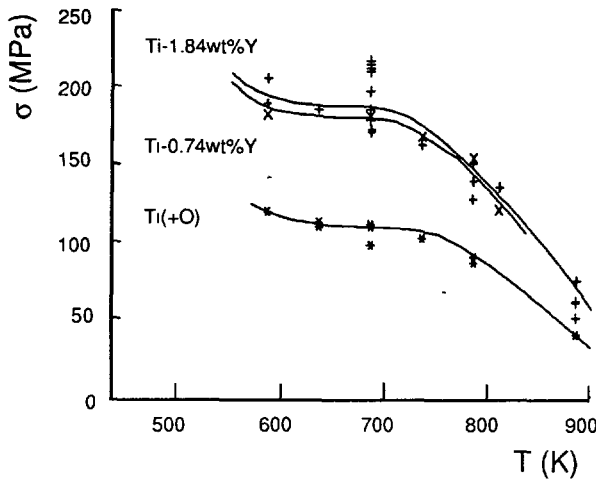


Fig. 2.

Fig. 2. — The temperature dependence of the yield stress in titanium containing 3 000 ppm of oxygen and in two Ti-Y alloys. Notice the plateau between 600 K and 700 K. After Perrier [12].

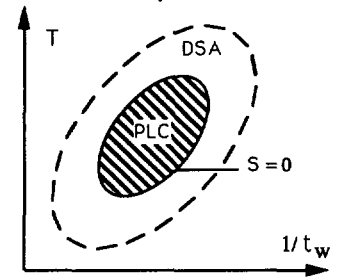


Fig. 3.

Fig. 3. — (Schematic) The domain of occurrence of dynamic strain ageing and of the PLC effect in the plane (inverse waiting time,  $t_w^{-1}$ ; temperature  $T$ ).

Therefore the slope of the total glide resistance vs. the strain rate, which is normally positive, is decreased and may even become negative within a range of waiting times or strain rates. It follows from figure 1 that the total strain rate sensitivity <sup>(1)</sup>,  $S = (\partial \sigma / \partial \ln \dot{\epsilon})_{\epsilon}$  is reduced by ageing effects and may become negative. The combination of ageing and activation mechanisms can be expressed in several different forms. In what follows we adopt the assumption [10] that the mentioned components of glide resistance are additive :

$$\sigma = \sigma_{\text{activation}} + \sigma_{\text{ageing}}(c, Dt_w) \tag{2}$$

<sup>(1)</sup> More strictly, the SRS is defined as the corresponding derivative taken at constant state [10]. The definition used here is, however, appropriate for constant strain rate testing followed by a strain rate jump test for which the « state » is represented by the plastic strain.

By combining eqs. (1) and (2) and eliminating the waiting time, one obtains a constitutive equation which serves as a basis for further modelling [2].

From these considerations we can draw a demarcation line between two related but different phenomena. Dynamic strain ageing can be considered effective when an anomaly appears in the flow stress *vs.* strain rate or temperature dependence, accompanied by a reduction in SRS. The anomaly in flow stress is thought to be responsible for the so-called plateau observed at medium temperatures in dilute alloys and impure metals (cf. Fig. 2 and below). As long as the SRS remains positive, plastic flow is uniform. Given the strain rate, the domain of the occurrence of DSA is limited by two temperatures, one below which the diffusion of solute atoms is too slow to allow for dynamic pinning, and the other at which the dislocation lines are permanently saturated with solute atoms. Thus, in the plane (inverse waiting time, temperature) the domain of the occurrence of DSA is indicated by the area enclosed by a « diffuse » boundary, as shown schematically in figure 3. This area may extend over several decades of waiting times.

Within the range of existence of DSA, the SRS may become negative which provides conditions for the occurrence of the PLC effect. Thus, the PLC effect is observed within a *subdomain* of the DSA domain. The boundary of this subdomain can be roughly represented by the condition  $S = 0$ , though in practice the onset of the PLC effect is often associated with  $S$  dropping below a finite negative value. Within the PLC domain deformation curves are serrated and in some favourable cases a propagating pattern of deformation bands can be visualized. The reader is referred to reference 2 for a detailed analysis of the relation between the SRS turning negative and the occurrence of plastic instabilities and strain localizations. Here, we just recall that as soon as this critical condition is fulfilled, any local fluctuation in strain rate is bound to increase in amplitude so that uniform plastic deformation is necessarily unstable.

A careful analysis is needed to characterize the occurrence of DSA when the SRS is positive. We illustrate this point by the two examples of figures 2 and 4. Figure 2 shows the temperature dependence of the yield stress in impure titanium and in two titanium alloys containing yttrium [11, 12]. Oxygen is known to be responsible for DSA and the PLC effect in impure Ti, and its total concentration in the non-alloyed Ti as well as in the alloys is about 3 000 ppm. More surprising is the observation of plateaus in the yield stress *vs.* temperature curves of the two alloys since most of the oxygen should be trapped by yttrium to form  $Y_2O_3$  particles. Actually there seems to be a small residual oxygen concentration in the matrix, which is estimated to be of the order of one to a few hundred ppm and this is apparently large enough to produce an observable effect.

Figure 4 shows the temperature dependence of the flow stress and of the SRS in an Al-Fe-V-Si alloy produced by rapid solidification techniques. There is a small anomaly in the flow stress *vs.* temperature dependence but the dip in SRS is a clear indication of the occurrence of DSA [13]. In « classical » aluminium alloys (e.g. alloys containing Mg, Cu, Zn...), the domain of the occurrence of DSA and of the PLC effect is centered around room temperature, while in the present case DSA appears close to 400 K. The reason is that the diffusing species is probably Fe, a transition element whose diffusivity in Al is much smaller than that of « normal » alloying elements. Although this is not quite apparent in figure 4, there is another SRS hole just below room temperature [14] which can only be caused by a « normal » diffusing element. This element can be identified with silicon which, indeed, has been shown recently to induce jerky flow in binary Al-Si alloys around room temperature [15].

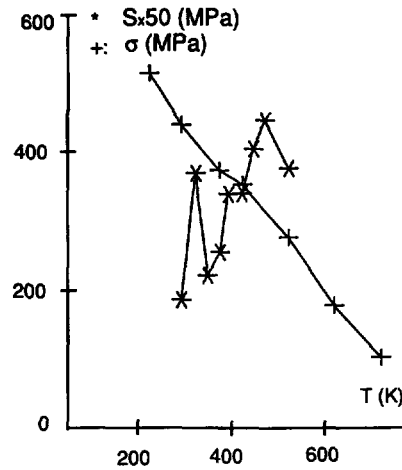


Fig. 4. — The temperature dependence of the yield stress,  $\sigma$ , and of the strain rate sensitivity,  $S$ , (measured at 2 % strain) in an Al-Fe-V-Si alloy drawn in the transverse direction with an applied strain rate of  $5 \times 10^{-5} \text{ s}^{-1}$ . Notice the reduction in strain rate sensitivity around 400 K and the slight hump in the flow stress above 400 K. After Bouchaud *et al.* [13].

### 3. Strain rate sensitivity and ductility.

At a phenomenological level, the ductility of a material can be understood in terms of two (evolutionary) quantities [16]: the strain hardening coefficient,  $h$ , or equivalently the reduced quantity  $n = h/\sigma$ , and the SRS,  $S$ , or the strain rate sensitivity index <sup>(2)</sup>  $m = S/\sigma$ . The SRS plays in a solid the role of the viscosity in a fluid: it opposes any increase in strain rate inside the material. Therefore, a high value of the SRS both promotes uniform deformation by delaying the onset of necking and inhibits the growth of strain localizations in the post-necking domain [17]. Conversely, a reduction in SRS, whatever its cause, may affect the ductility in two different ways. If the SRS is positive but small, the tendency to localization and the growth rate of heterogeneities will be enhanced. If the SRS becomes negative, the specimen is able to deform at increasing strain rates under decreasing stresses, i.e. spontaneous localization occurs. These qualitative arguments are not easily brought into analytic form because  $h$  as well as  $S$  usually evolve with strain and the post-localization behaviour involves multiaxial stress states.

Figure 5, reproduced from reference [18] illustrates very clearly the correlation which exists between the strain at rupture and the strain rate sensitivity index  $m$  in non-strain hardening materials ( $h = 0$ ). In figure 6 are plotted several calculated engineering stress-strain curves at a constant cross-head speed for model sheet specimens whose constitutive equation is defined

<sup>(2)</sup> This notation, common in the literature on formability is at variance with the one used in constitutive modelling where the inverse quantity is usually denoted by  $m$ .

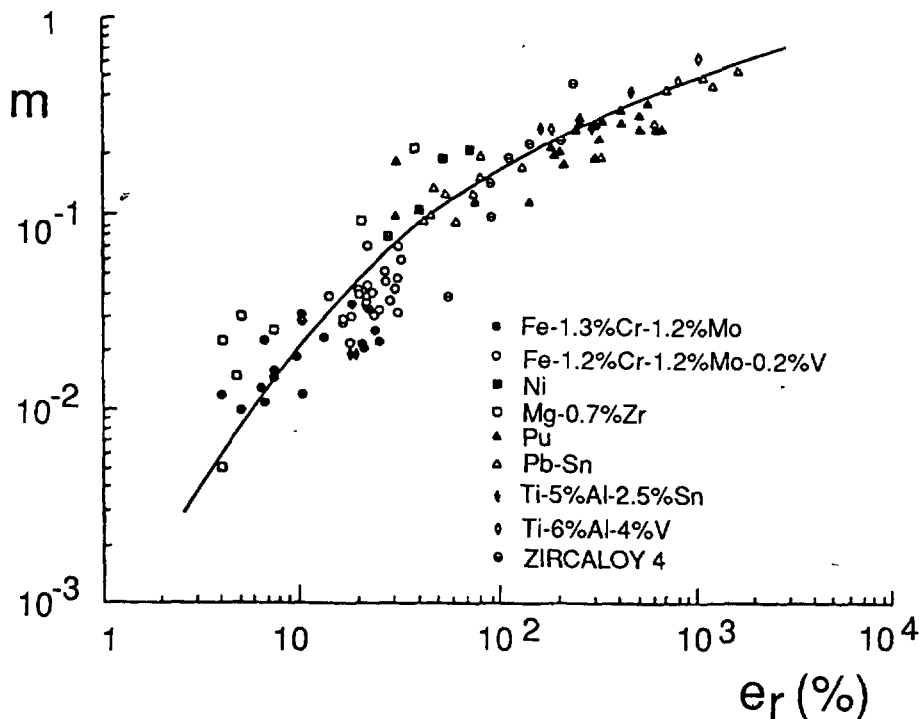


Fig. 5. — Correlation between the strain rate sensitivity index  $m$  and the elongation at rupture,  $e_r$ , for a variety of materials. After Woodford [16].

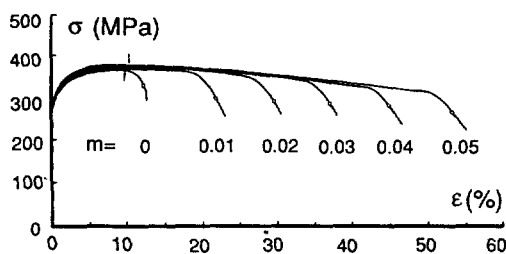


Fig. 6. — The dependence of the calculated engineering stress-strain curves on the value of the strain rate sensitivity index  $m$ , for sheet specimens containing an initial imperfection. The arrows indicate the position of the maximum load. After Ghosh [17].

through two coefficients  $m$  and  $n$  [19]. Here  $m$  is variable,  $n = 0.1$  and the specimens initially contain a small geometric imperfection. For increasing positive values of  $m$  a very significant increase in elongation is obtained beyond the maximum load. In the same work and for slightly negative values of  $m$ , serrations were obtained on the deformation curves at and beyond the maximum load. For sufficiently negative values of  $m$  it was found that the uniform strain may reduce to values lower than  $n$ , in some analogy with Hart's criterion [20].

Generally, it can be expected that the effect of the negativeness of the SRS should be qualitatively different from the one predicted by just extrapolating the plots of figure 6 into the negative region. Indeed, the very character of plastic deformation changes here from uniform to band-like. Thus, with regard to DSA mechanisms, we see that the resulting decrease in SRS within a certain temperature range must be accompanied by a reduction of the elongation to rupture, the effect being larger in the PLC range. This seems to be the most convincing explanation for a ductility dip found in many alloys at intermediate temperatures. As an example, figure 7 shows the elongation to rupture of a rapidly solidified Al-Cr-Zr alloy as a function of temperature (after [13]). A « ductility hole » occurs near 500 K, while the SRS, as measured at 1 % strain, exhibits a minimum at 450 K, indicating a correlation. The concentrations of Cr and Zr dissolved in the aluminium matrix were measured by atom-probe microanalysis and both were of the order of 0.3 at%, i.e., values which are certainly sufficient to induce DSA. Therefore, in such alloys DSA effects, which are caused by slow-diffusing transition elements, tend to reduce the ductility precisely in the domain of temperatures of practical interest.

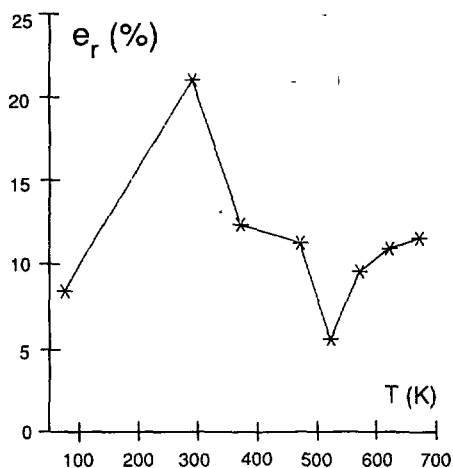


Fig. 7. — The total elongation at rupture,  $e_r$ , vs. temperature in an Al-Cr-Zr alloy strained in the long direction with an applied strain rate of  $5 \times 10^{-5} \text{ s}^{-1}$ . Notice the ductility hole around 500 K. After Bouchaud *et al.* [13].

This embrittlement effect of DSA, which is similar to the « blue brittleness » of steels [21], should be expected to be observed in most modern aluminium alloys like the rapidly solidified alloys containing dissolved transition elements well above the solubility limit or the aluminium-lithium alloys which will be considered below. Unfortunately, few detailed analyses taking into account DSA effects or investigating strain rate effects have been performed for these materials to date. Thus, we conclude this section with an example drawn from a classical alloy [22]. Figure 8 shows the strain rate dependence of the ultimate tensile stress of an Al-Zn-Mg alloy at several temperatures. At the liquid nitrogen temperature the

rate sensitivity is positive and it turns negative at and slightly above room temperature which is accompanied by the appearance of serrations on the deformation curves and by a decrease of the elongation to rupture. Figure 9, reproduced from the same work, shows the displacement vs. time curve of a notched specimen of Al-Zn-Mg during a bend test performed at room temperature and at a constant loading rate. A stepped deformation curve is characteristic of the PLC effect with constant loading rate and the last elongation burst leads to a catastrophic type of shear failure. This particular rupture mode occurs at or just beyond the maximum load and appears to be connected with continued activity in the PLC bands ahead of the notch.

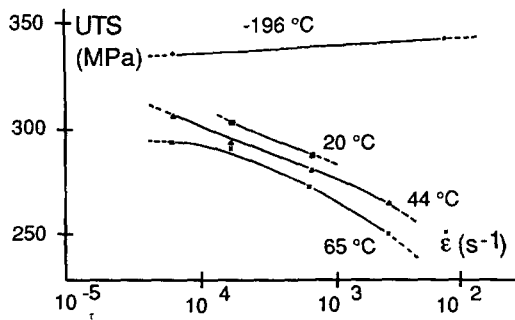


Fig. 8.

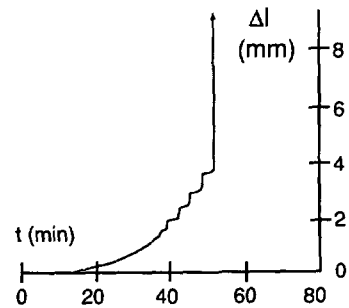


Fig. 9.

Fig. 8. — The strain rate dependence of the ultimate tensile stress in Al-Zn-Mg specimens at various temperatures. The negative slopes are associated with jerky flow. After King, You and Knott [21].

Fig. 9. — Displacement vs. time curve at room temperature for an Al-Zn-Mg notched specimen tested in bending with a constant loading rate at room temperature. After King, You and Knott [22].

#### 4. Strain effects.

Strain effects are inherent in the mechanisms of dynamic and static *strain* ageing. Figure 10 shows the strain dependence of the SRS in impure titanium (which is further referred to as Ti-O), after Perrier [12]. At 773 K, the SRS monotonically increases with strain, which is a « normal » behaviour in the absence of DSA. (In fcc metals, for instance, the SRS is proportional to the flow stress which dependence is referred to as the Cottrell-Stokes law.) At 673 K, the SRS first decreases, passes through a minimum and then increases. This initial decrease in SRS, which has been observed in many substitutional and interstitial alloys, and which may extend over large strain intervals (0.1-0.2), is characteristic of DSA and indicates that ageing effects are enhanced by plastic strain.

A similar effect is observed during static strain ageing tests. During such tests, the specimen is unloaded and maintained under zero stress during a prescribed time interval. Upon reloading, a yield point is observed whose amplitude increases with both ageing time and prestrain (or flow stress). This is illustrated by figures 11 and 12 which refer to two interstitial alloys : Ni-C [23] and Ti-O [12], respectively. The relation between static and dynamic strain ageing is simply that in the first case the ageing time is prescribed, while in the second one the waiting time is indirectly prescribed by the plastic strain rate.

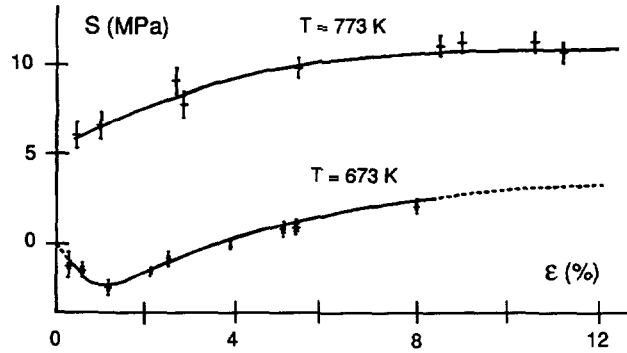


Fig. 10. — Strain dependence of the strain rate sensitivity in Ti-O. After Perrier [12].

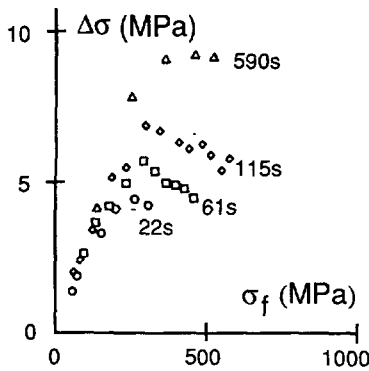


Fig. 11.

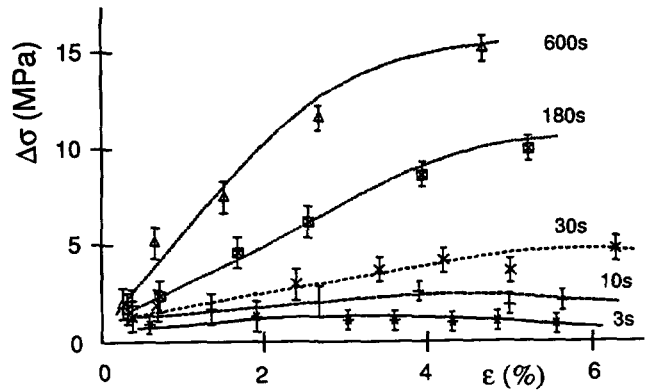


Fig. 12.

Fig. 11. — Flow stress dependence of the stress increment upon static ageing in a Ni-0.2 at.%C alloy for several ageing times at 453 K. After Kocks, Cook and Mulford [23].

Fig. 12. — Strain dependence of the static ageing peak in Ti-O for several ageing times at 673 K. After Perrier [12].

According to the classical models, these strain effects can be explained by the increase in vacancy supersaturation caused by plastic flow which enhances the diffusivity of solute atoms. However, as first noticed by Kocks, Cook and Mulford in their investigation of a Ni-C alloy [23], vacancies play no role in the diffusion of interstitial atoms while the strain dependence is still present (cf. Figs. 11 and 12). In the model proposed by Mulford and Kocks [9], it is assumed that ageing effects influence the strength of the dislocation-dislocation interactions, rather than the interaction between solute atoms and dislocations.

There seems to be, however, a simpler explanation which relies on the strain dependence of the densities of mobile and forest dislocations [24]. These two densities come into play through the quantity  $\Omega = b\rho_m \rho_f^{-1/2}$ , defined in section 2 (cf. Eq. (1)). A typical strain dependence of  $\Omega$  is represented in figure 13, where typical numerical values are indicated. This non-monotonic behaviour can be understood as follows: at small strains, the strain dependence of  $\Omega$  is essentially governed by a strong increase in the density of mobile dislocations. At larger strains, the mobile density progressively saturates while the forest density further increases and then saturates in its turn.  $\Omega$  passes through a maximum and then

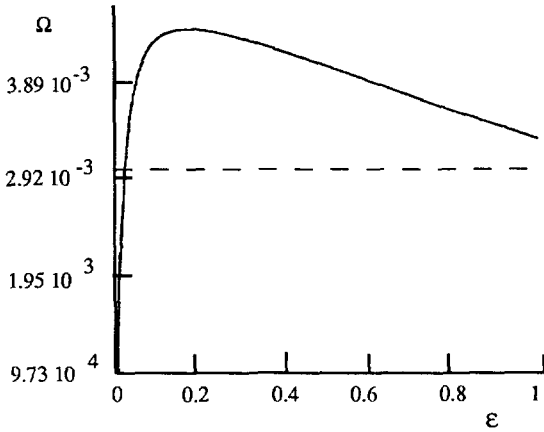


Fig. 13.

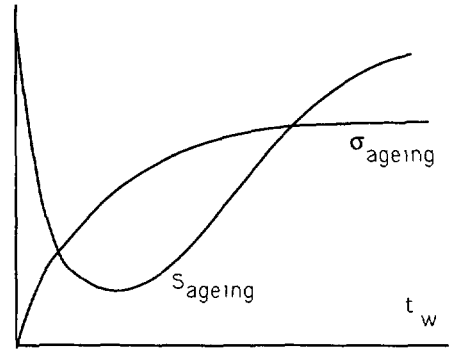


Fig. 14.

Fig. 13. — Strain dependence of the elementary strain increment  $\Omega$  obtained when all mobile dislocations perform a successful thermally activated jump. The dotted line indicates the asymptotic value reached at large strains. Numerical values are typical of an aluminium alloy at room temperature.

Fig. 14. — The dependence of the ageing components of the glide resistance and of the strain rate sensitivity on the waiting time  $t_w$  (schematic).

asymptotically reaches a saturation value. During plastic flow a constant strain rate is usually prescribed. Assuming the plastic strain rate to be constant, the waiting time must have, within a proportionality factor, the same strain dependence as  $\Omega$ . The ageing component of the flow stress,  $\sigma_{ageing}$ , has a dependence on waiting time which is schematically represented in figure 14: it increases and saturates for large waiting times. Thus  $\sigma_{ageing}$  increases with strain until  $\Omega$  passes through its maximum value and then it decreases towards a saturation value. This is basically the behaviour obtained in figures 11 and 12 where a slight decrease of the ageing peak is observed at large strains.

In figure 14 is also plotted the dependence of the ageing component of the SRS on the waiting time, as given by :

$$S_{ageing}(t_w) = (\partial \sigma_{ageing} / \partial \ln \dot{\epsilon})_{\epsilon} = - d \sigma_{ageing} / d \ln t_w . \tag{3}$$

This dependence is nonmonotonic, so that the strain dependence of the SRS which includes two nonmonotonic dependences [ $S(t_w)$  and  $t_w(\epsilon)$ ] may have different shapes according to the experimental conditions. Most common is the situation depicted in figure 10: the SRS first decreases getting negative and further increases with increasing strain. An upper bound of the PLC range corresponds to the strain at which  $S$  turns positive again. A more peculiar case is met when  $S_{ageing}(\epsilon)$  exhibits two minima, so that two separated PLC ranges are possible. It provides a critical check for the present interpretation of strain effects through the investigation of the critical strains for the onset and disappearance of jerky flow on deformation curves [2].

Figure 15 reproduces serrated stress-strain curves obtained at room temperature for a quaternary Al-Li-Cu-Mg alloy. As already mentioned, the critical conditions for a bifurcation from uniform to nonuniform flow (or *vice versa*) are met when the strain is such that the total SRS passes through zero (or as already mentioned, attains a small negative value). We

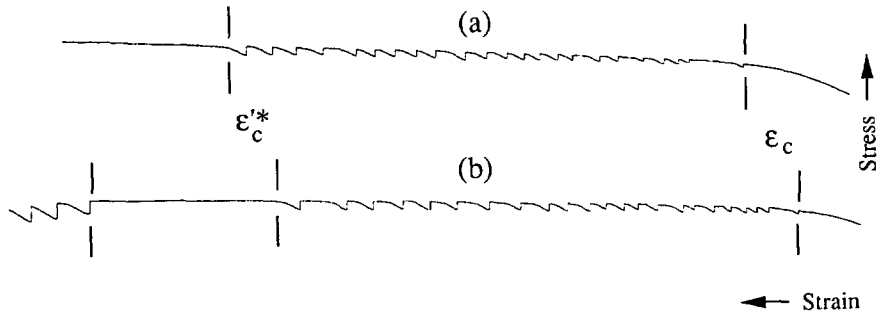


Fig. 15. — Serrated deformation curves in an Al-Li-Cu-Mg alloy at room temperature: a) A stress-strain curve exhibiting a lower and an upper critical strain ( $\dot{\epsilon} = 1.75 \times 10^{-5} \text{ s}^{-1}$ ), b) A curve showing two regions of jerky flow separated by a smooth region ( $\dot{\epsilon} = 2 \times 10^{-5} \text{ s}^{-1}$ ). After [2].

express the critical condition by setting  $S$  equal to zero :

$$S_0 + S_{\text{ageing}}(\epsilon_c) = 0. \quad (4)$$

Since  $S_{\text{ageing}}(\epsilon)$  may have two distinct minima, the number of critical strains can in theory be as large as four, although in practice some of the critical strains may be too small or too large to be recorded. In figure 15b, three critical strains are obtained and a small domain of uniform flow, which is very sensitive to temperature and strain rate, is observed at large strains. Other examples and an investigation of all the possible cases and of their dependence on experimental conditions (solute concentration, temperature, strain rate) are given in reference [24]. It follows from this model that the strain dependences of static and dynamic strain ageing can be qualitatively described in full detail without involving any assumption of a possible effect of deformation-induced vacancies. The nature of the diffusional mechanism of substitutional solutes has not been completely clarified, however, and contradictory evidences are still being debated.

### 5. Strain rate effects.

Several effects arise from the anomalous strain rate dependence of  $\sigma_{\text{ageing}}$  and  $S_{\text{ageing}}$  (cf. Figs. 1 and 14), which we report here without going into detail. Because  $\sigma_{\text{ageing}}$  is strongly strain rate-dependent, the experimental measurement of the SRS, e.g. through a strain rate change, depends on the values of the initial and final strain rates as shown by Diehl, Springer and Schwink [25]. In addition, transient effects appear during upwards strain rate changes which are due to the fact that the equilibrium solute concentration on dislocation lines cannot instantaneously adjust to the new strain rate [26]. As a result, the apparent SRS which is experimentally measured in conditions of dynamic strain ageing differs from the « true » SRS. For instance in figure 10 the apparent SRS of the Ti-O alloy becomes negative at 673 K within a small strain interval. No serrated flow is however recorded in this interval. This is in accord with the statement that the (apparent) SRS must drop below a small negative value for jerky flow to occur.

The measurements of the SRS during jerky flow also lead to some difficulties and controversies [27, 28], although it is now widely recognized that microscopically meaningful values cannot be measured directly since they correspond to unstable dislocation states. What is measured in practice is the response of the critical stress for a stress drop or of the depth of the drops (serration amplitude) to a change in strain rate. These two quantities have similar

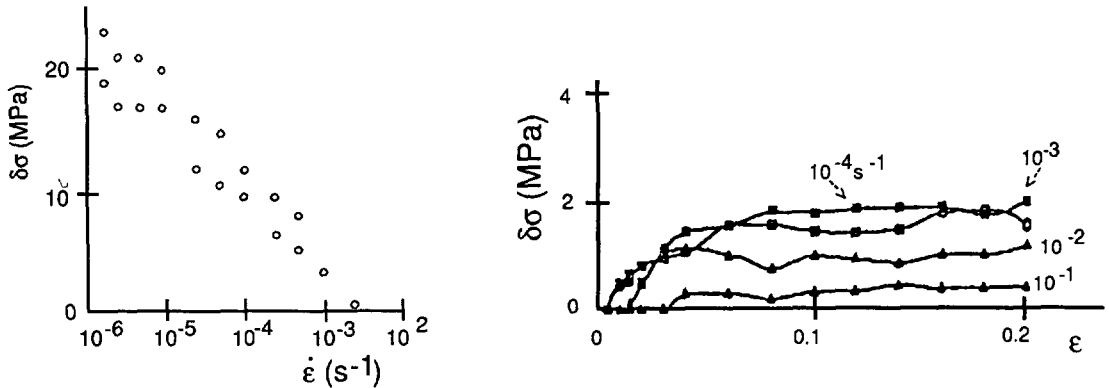


Fig. 16. — The strain rate dependence of serration amplitude,  $\delta\sigma$ , in an Al-Mg alloy strained at room temperature. After [30].

Fig. 17. — The strain dependence of PLC serrations in a quaternary Al-Li-Cu-Zr alloy for various applied strain rates. A vertical section of these curves yields a strain rate dependence similar to the ones of figures 16, 18 and 20. After Huang and Gray [31].

strain rate dependences because the lower stress level of serrations, which corresponds to the repinning of mobile dislocations by solute atoms, is rather constant.

As has been shown in section 2 (cf. Fig. 2) jerky flow occurs, at a given temperature, within a range of strain rates. Most of the experimental observations, starting with the work of Cuddy and Leslie [29] on substitutional solutions of iron, show a very characteristic behaviour. When the strain rate is increased from low values in the stable domain, serrated flow sets in abruptly with a large amplitude. With increasing strain rate, this amplitude remains rather constant or slowly decreases but further drops rather steeply. At the upper strain rate limit, jerky flow disappears with a vanishing amplitude. This is illustrated by figure 16, in the case of a classical alloy, Al-Mg, [30] and by figure 17 which is reproduced from a recent study on quaternary Al-Li based alloys [31]. In both figures 16 and 17, the serration amplitude appears to have a negative strain rate sensitivity.

This effect can be understood as follows [32]. During the reloading which follows a stress drop, the specimen is being strained uniformly and its deformation is partly elastic and partly plastic. The effective stress on mobile dislocations increases with time and its variation during a waiting time can no longer be neglected at high applied strain rates. In addition to the mechanisms of activation and ageing (cf. Fig. 1), one has to take into account this « loading » effect. At low strain rates, the influence of loading is negligible and the critical stress for breaking through the forest obstacles is almost strain rate independent. As the strain rate increases, the increase in effective stress during a waiting time progressively prevails over the increase in glide resistance produced by ageing, and the critical stress for the amplitude of a serration decreases. At the upper limit of the PLC domain, breaking through the forest obstacles occurs by dislocations denuded of their solute atmospheres since only a vanishingly small concentration of solute atoms can accumulate on the dislocation lines within the correspondingly small waiting times.

Quite interestingly, a very similar phenomenon seems to be associated with stick-slip mechanisms. Stick-slip instabilities derive from the particular dynamic properties of dry friction [33]. The friction stress opposing the sliding of two surfaces past each other depends

on the relative sliding velocity : for small sliding velocities, dynamic friction decreases below the level of static friction and further increases for larger velocities. Within a certain domain of velocities, the sensitivity of the friction stress to the velocity is negative and the relative displacement of the two surfaces is jerky. This instability mechanism belongs to the same general class (relaxation oscillations) as the one associated with the PLC effect [34]. Stick-slip has been observed in particular in composite materials (see [35] and references therein), in cases where the (hard) fibers have to accommodate the plastic deformation of a ductile matrix by interfacial glide. To investigate this phenomenon, experiments have recently been performed [35] on a model composite material, made of a copper wire embedded in a cylindrical epoxy matrix. Figure 18 shows a plot of the stick-slip amplitude as a function of the velocity with which the wire is pulled out from the matrix. The striking similarity with the effect discussed above (see also Fig. 20 below) is not understood to date.

Finally, figures 19 and 20 are reproduced from the work of Gentzbittel [36] on the cyclic deformation of a binary Al-Li alloy. The stress-strain cycle exhibits distinct serrations, whose amplitude is plotted in figure 20 as a function of the applied strain rate. It seems, of course, attractive to interpret this behaviour as a manifestation of the PLC effect caused by the diffusion of Li atoms [37, 38, 31]. An alternative explanation has, however, been proposed [36]. There is experimental evidence that a softening mechanism associated with the repeated shearing and dissolution of  $\delta'$  ( $\text{Al}_3\text{Li}$ ) coherent particles induces strong localizations of plastic flow [39] which can be held responsible for the occurrence of serrations. At low strain rates, the dissolved species have time to precipitate during reloading so that the critical stress for the onset of localized slip is not strain rate dependent. At larger strain rates, the loading effect gets faster than precipitation so that the bands get increasingly softer with increasing strain rates. Therefore, this model may be considered as a variant of a DSA mechanism where precipitation replaces ageing effects, while loading and activation mechanisms are still operative. The net result is the same as that discussed above, *viz.* a negative apparent SRS. This example, which is not discussed here in full detail, illustrates some difficulties often met with advanced materials. The improvement of strength, e.g. through precipitation hardening, results in the presence of elements dissolved in the matrix. The concentration of these elements depends on prior treatments and is not precisely known, except if atom-probe microanalysis can be performed. As a result, both strain and strain rate softening mechanisms can cooperate to significantly reduce the ductility.

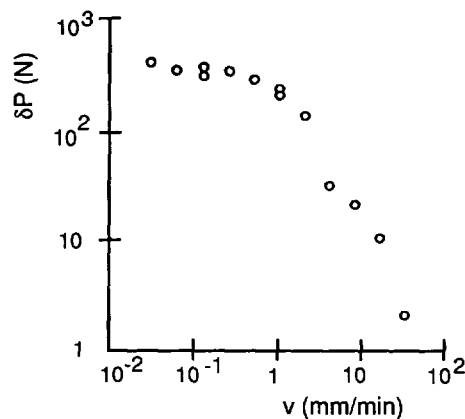


Fig. 18. — The dependence of load drop amplitude,  $\Delta P$ , on cross-head velocity,  $v$ , during the pull-out of a fiber in a model composite material. After Cook *et al.* [35].

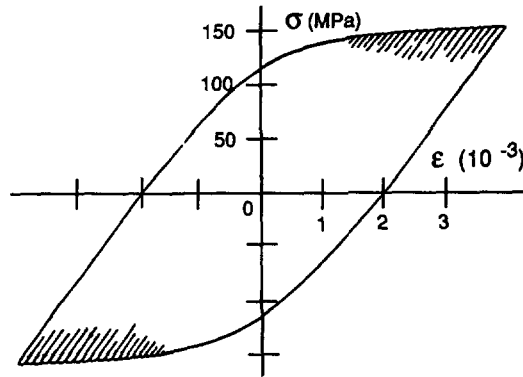


Fig. 19. — A deformation cycle exhibiting instabilities during the fatigue of a binary Al-Li alloy at room temperature and with a constant plastic strain amplitude of  $\Delta\varepsilon_p/2 = 2 \times 10^{-3}$  After Gentzbittel [36].

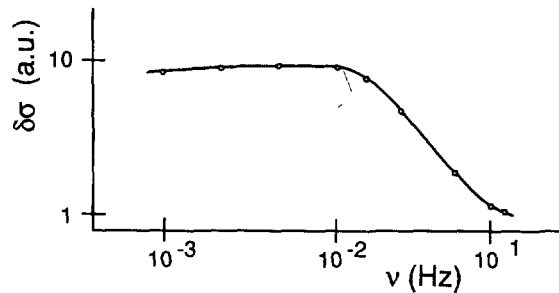


Fig. 20. — Frequency dependence of the amplitude of the instabilities shown in figure 19. After Gentzbittel [36].

## 6. Concluding remarks.

Although the arguments presented here are essentially qualitative, they can be brought into semi-quantitative form. The main features associated with static and dynamic strain ageing are now reasonably understood owing to a synergy between the continuation of fundamental studies and the emergence of new classes of alloys with an increased demand for a better control of mechanical properties. Emphasis has been put on the detrimental effect of DSA on the ductility of alloys and on the characteristic strain and strain rate dependences which can be used for characterizing these phenomena. An item which has not been examined to date is a possible correlation between loss of fracture toughness and DSA. It should be addressed in future studies aiming at designing novel high-performance materials.

## References

- [1] NEUHÄUSER H., PLESSING J. and SCHÜLKE M., *Mech. Behav. Mater.* **2** (1989) 231-254.
- [2] ESTRIN Y. and KUBIN L. P., *J. Mech. Behav. Mater.* **2** (1989) 255-292.
- [3] COTTRELL A. H., *Dislocations and Plastic flow in solids* (Clarendon Press, Oxford) 1953.
- [4] FRIEDEL J., *Dislocations* (Pergamon Press, Oxford) 1967.
- [5] MCCORMICK P. G., *Acta Metall.* **20** (1972) 35.
- [6] VAN DEN BEUKEL A., *Phys. Status Solidi (a)* **30** (1975) 197.
- [7] SLEESWIJK A. W., *Acta Metall.* **6** (1958) 598.
- [8] MULFORD R. A. and KOCKS U. F., *Acta Metall.* **27** (1979) 1125.
- [9] VAN DEN BEUKEL A. and KOCKS U. F., *Acta Metall.* **30** (1982) 1027.
- [10] KOCKS U. F., *Prog. Mater. Sci.*, Chalmers Anniversary Volume (Pergamon Press, Oxford) 1981.
- [11] PERRIER Ch., NAKA S. and KUBIN L. P., *Scr. Metall.* **23** (1989) 477.
- [12] PERRIER Ch., Doctorate Thesis, Université Pierre et Marie Curie, Paris 1989.
- [13] BOUCHAUD E., KUBIN L. and OCTOR H., *Metall. Trans.*, in press.
- [14] SKINNER D. J., ZEDALIS M. S. and GILMAN P., *Mater. Sci. Eng. A* **119** (1989) 81.
- [15] NIINOMI M., KOBAYASHI T. and IKEDA K., *J. Mater. Sci. Lett.* **5** (1986) 1081.
- [16] MATLOCK D. K. and KRAUSS G., *Formability and Metallurgical Structure*, ed. A. K. Sachdev and J. D. Embury (The Metallurgical Society) 1987, p. 33.
- [17] KOCKS U.F., JONAS J. J. and MECKING H., *Acta Metall.* **27** (1979) 419.
- [18] WOODFORD D. A., *Trans. ASM* **62** (1969) 291.
- [19] GHOSH A. K., *Metall. Trans.* **8A** (1977) 1221.
- [20] HART E. W., *Acta Metall.* **15** (1967) 351.
- [21] GROOM J. D., Ph. D. Thesis, University of Cambridge (1971).
- [22] KING J. E., YOU C. P. and KNOTT J. F., *Acta Metall* **29** (1981) 1553.
- [23] KOCKS U. F., COOK R. E. and MULFORD R. A., *Acta Metall.* **33** (1985) 623.
- [24] KUBIN L. P. and ESTRIN Y., *Acta Metall.* **38** (1990) 697.
- [25] DIEHL L., SPRINGER F. and SCHWINK Ch., *Strength of Metals and Alloys 1 (ICSMA 8)*, ed. P. O. Kettunen *et al.* (Pergamon Press, Oxford) 1988, p. 313.
- [26] MCCORMICK P. G. and ESTRIN Y., *Scr. Metall.* **23** (1989) 1231.
- [27] DYBIEC H., *Scr. Metall.* **22** (1988) 595.
- [28] KUBIN L. P. and ESTRIN Y., *Scr. Metall.* **23** (1989) 815.
- [29] CUDDY L. J. and LESLIE W. C., *Acta Metall.* **20** (1972) 1157.
- [30] CHIHAB K., ESTRIN Y., KUBIN L. P. and VERGNOL J., *Scr. Metall.* **21** (1987) 2707.
- [31] HUANG J. C. and GRAY G. T., *Scr. Metall.* **24** (1990) 85.
- [32] KUBIN L. P., CHIHAB K. and ESTRIN Y., *Acta Metall.* **36** (1988) 2707.
- [33] STOKER J. J., *Nonlinear vibrations 2* (Interscience, N.Y.), 1950.
- [34] KUBIN L. P. and POIRIER J. P., *Non Linear Phenomena in Materials Science*, ed. L. P. Kubin and G. Martin (Trans Tech Publications) 1988, p. 473.
- [35] COOK R. F., THOULESS D. R., CLARKE D. R. and KROLL M. C., *Scr. Metall.* **23** (1989) 1725.
- [36] GENTZBITTEL J. M., Doctorate Thesis, INSA Lyon (1988).
- [37] DAMERVAL C., LAPASSET G. and KUBIN L. P., *Aluminium-lithium alloys 2*, Eds. T. H. Sanders and E. A. Starke (Materials and components, Eng. Publications) 1989, p. 859.
- [38] MIURA Y., NISHITANI S., FURUKAWA M. and NEMOTO M., *Strength of Metals and Alloys 2 (ICSMA 8)* Eds. P. O. Kettunen *et al.* (Pergamon Press, Oxford) 1988, p. 995.
- [39] BRECHET Y., LOUCHET F., MARCIONI Ch. and VERGER-GAUGRY J. L., *Phil. Mag. A* **56** (1987) 353.